Determination of electron-phonon interaction parameters from time-domain terahertz spectroscopy

M. A. Gilmore, Saeid Kamal, D. M. Broun, and J. S. Dodge[a)]
Department of Physics, Simon Fraser University, Burnaby, British Columbia V5A 1S6, Canada

(Received 7 November 2005; accepted 8 March 2006; published online 4 April 2006)

We present an analytical framework for determining metallic electron-phonon interaction parameters from time-domain terahertz spectroscopy measurements. We apply this analysis to the case of lead, where we obtain values that are consistent with existing estimates. We discuss the statistical and systematic errors that limit the uncertainty in the parameter estimates. © *2006 American Institute of Physics*. [DOI: 10.1063/1.2192625]

The theory of electron-phonon interactions relies on a function $\alpha^2F(\omega)$ that jointly characterizes the electron-phonon coupling and the phonon density of states.[1] A variety of methods exists for determining $\alpha^2F(\omega)$ experimentally,[2,3] but most physical phenomena can be characterized by a relatively small set of parameters that derive from it; often, it is easier and more reliable to measure these parameters directly. We have developed a method that employs time-domain terahertz spectroscopy (TDTS) to determine two such parameters: the transport-weighted electron-phonon coupling constant λ_{tr}, and a parameter T_0 that controls the overall temperature dependence of the electron-phonon mass enhancement. The method also determines a third parameter that relates to the purely electronic degrees of freedom in the metal, the plasma frequency ω_p. We present below the general features of the method, and discuss its application to thin-film samples of lead, for which we obtain parameter values that are in good agreement with the independent measurements. The method may be used to measure electron-boson interactions in any metal film.

The raw data for our analysis are measurements of two sets of picosecond electromagnetic pulses, generated and sampled on a subpicosecond time scale with photoconducting switches and a femtosecond laser.[4] Examples of the pulses and their Fourier amplitudes are shown in Fig. 1. One pulse, $E_s(t)$, is measured after transmission through a thin-film sample of the material of interest. The other pulse, $E_r(t)$, is measured after transmission through a transparent reference substrate that is matched to that of the sample. We attach both the sample and reference to a moveable sample holder inside an optical cryostat, and measure reference and sample pulse pairs for a range of temperatures. We use a discrete Fourier transform (dFT) to determine the complex field amplitudes, $\tilde{E}_{ri} \equiv \tilde{E}_r(\omega_i)$ and $\tilde{E}_{si} \equiv \tilde{E}_s(\omega_i)$, and thereby determine the relative transmission amplitude,

$$\tilde{t}_{sr}(\omega_i) = \frac{1}{1 + \kappa\tilde{\sigma}(\omega_i)/\sigma_0} e^{i\omega_i\eta}, \quad (1)$$

valid when the metallic film is much thinner than the skin depth. In this expression, $\kappa = \sigma_0 d Z_0/(n+1)$ is a dimensionless constant that relates the dc conductivity σ_0 and thickness d of the sample film, the impedance of free space Z_0, and a frequency-independent substrate refractive index n, assumed identical for both the sample and the reference. We include a temporal delay η to account for the possibility that the optical thicknesses of the sample and reference substrates are not perfectly matched. Information concerning electron-phonon mass enhancement is contained in the complex conductivity of the sample, $\tilde{\sigma}(\omega)$.

In the low-frequency limit of the conventional electron-phonon theory of metals,[5–7] we can express the conductivity as

$$\tilde{\sigma}(\omega,T) = \frac{\sigma_0(T)}{1 - i\omega\tau^*(T)}, \quad (2)$$

where $\tau^*(T) = \tau(T)[1+\lambda(T)]$ is the relaxation time for the dc conductivity, *renormalized* by a factor of $1+\lambda(T)$ due to the electron-phonon interaction. This renormalization is unobservable in the dc conductivity, $\sigma_0 = \epsilon_0\omega_p^2\tau$, because the

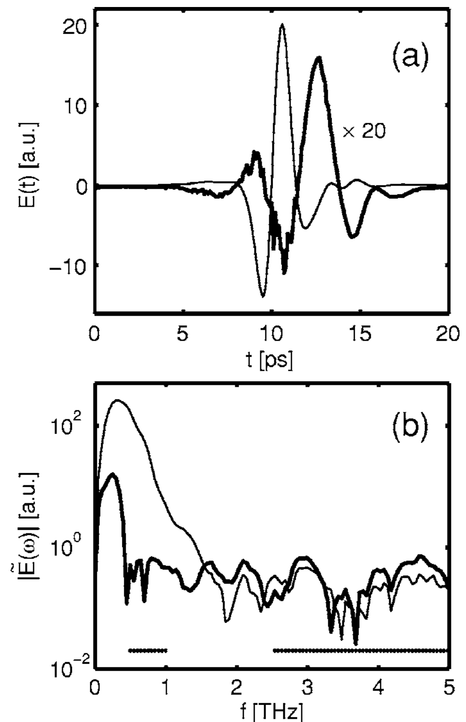

FIG. 1. Sample pulse (thin lines) and residuals (thick lines) in (a) the time domain and (b) the frequency domain. The sample temperature is 295 K. The time-domain residuals are scaled up by a factor of 20, and the points used in the fit and for the noise estimate are indicated by markers at the bottom of (b).

a)Electronic address: jsdodge@sfu.ca

 © 2006 American Institute of Physics
Downloaded 05 Apr 2006 to 142.58.211.84. Redistribution subject to AIP license or copyright, see http://apl.aip.org/apl/copyright.jsp

renormalization of ω_p^2 cancels that of τ.[8] In principle, $\lambda(T)$ must be calculated from $\alpha^2F(\omega)$, but a simple parametric form,

$$\lambda(T) = \frac{\lambda_{\text{tr}}}{1+(T/T_0)^2}, \tag{3}$$

is adequate for describing many measurements, as Shulga has emphasized.[7]

We can further simplify the model by noticing that when our frequency bandwidth is much smaller than the renormalized scattering rate $1/\tau^*$, the model given by Eqs. (1) and (2) is indistinguishable from the model

$$\tilde{t}_{sr}(\omega,T) = \alpha(T)e^{i\omega\xi(T)}, \tag{4}$$

where $\alpha=1/(1+\kappa)$, and $\xi=\eta-\kappa\tau^*/(1+\kappa)$. In this form, it is clear that the amplitude of $\tilde{t}_{sr}$ relates to the dc conductivity of the film, while its phase is linearly related to τ^*. Moreover, η and τ^* are not separately identified in a fit to this model, so any uncertainty in η directly affects our knowledge of τ^*. If the relaxation rate is low enough compared to the bandwidth, then it is possible to identify these parameters separately by fitting to Eq. (1), but they will remain highly correlated. For most metallic systems, the model in Eq. (4) is sufficient.

Using Eqs. (1)–(4), we can determine λ_{tr}, T_0, ω_p, η, and $\tau(T)$ from measurements of the sample and reference pulses over a range of temperatures. In the TDTS literature, it is common to treat $\tilde{E}_{si}/\tilde{E}_{ri}$ as the measured $\tilde{t}_{sr}(\omega_i)$, and invert Eq. (1) to obtain conductivity measurements; a least-squares fit of the conductivity model to the transformed data then determines the model parameters. It is important to recognize, however, that $\tilde{E}_{ri}$ and $\tilde{E}_{si}$ both contain noise, so transformations of this type can amplify noise and bias parameter estimates.[9] The extremely high signal to noise ratio of TDTS allows this procedure to work reasonably well in most cases, but it is difficult to determine parameter uncertainties precisely, as the weights and frequency range used in the fit are often governed by arbitrary choices.

We use a maximum likelihood (ML) framework to guide our analysis and put it on more secure footing.[10] We assume that the raw dFT spectra are related to an ideal pulse spectrum $\mathcal{E}_i$ in the following relationship:

$$\tilde{E}_{ri} = \tilde{\mathcal{E}}_i + \varepsilon_{ri}, \tag{5a}$$

$$\tilde{E}_{si} = \tilde{t}_{sr}(\boldsymbol{\theta};\omega_i)\tilde{\mathcal{E}}_i + \varepsilon_{si}, \tag{5b}$$

where $\tilde{t}_{sr}(\boldsymbol{\theta};\omega_i)$ is the relative transmission amplitude at ω_i, parameterized by the vector $\boldsymbol{\theta}$; in this case $\boldsymbol{\theta}=[\alpha,\xi]$ at a particular temperature T. The $\varepsilon_{(r,s)i}$ represent noise terms, assumed to be Gaussian random variables with standard deviations $\sigma_{(r,s)}$ independent of frequency. In our system, these assumptions are satisfied approximately; deviations from Gaussian white noise can be readily accommodated by incorporating the covariance matrices of $\varepsilon_{(r,s)i}$.[10] The ML estimator $\hat{\boldsymbol{\theta}}$ for the parameter vector is given by minimizing[11,12]

$$C(\boldsymbol{\theta}) = \frac{1}{2}\sum_i \frac{|\tilde{E}_{si}-\tilde{t}_{sr}(\boldsymbol{\theta};\omega_i)\tilde{E}_{ri}|^2}{\sigma_s^2+|\tilde{t}_{sr}(\boldsymbol{\theta};\omega_i)|^2\sigma_r^2}. \tag{6}$$

In general, the raw time-domain data used in TDTS are oversampled, so we can reliably estimate the uncertainties $\sigma_{(r,s)}$ by examining the dFT spectra outside the signal bandwidth.

Equation (6) provides a well-defined method for evaluating the goodness of fit. If we use high frequencies to determine empirical noise estimates $\hat{\sigma}_{(r,s)}$, Monte Carlo simulations indicate that the resulting distribution for $C(\boldsymbol{\theta})$ approximately follows an F distribution.[10] If there are N_f frequencies used for the fit, N_n frequencies for the noise estimates, and N_p free parameters in $\boldsymbol{\theta}$, we can evaluate the fit by comparing $C(\boldsymbol{\theta})$ to $F(x/2\nu_1;\nu_1,\nu_2)$, where $\nu_1=N_f-N_p$ and $\nu_2=2N_n-2$. A further benefit of Eq. (6) is that the statistical uncertainty in the parameter vector can be estimated directly from the covariance matrix $\mathbf{V}=(\mathbf{J}^T\mathbf{J})^{-1}$, where $\mathbf{J}$ is the Jacobian matrix of $C(\boldsymbol{\theta})$ evaluated at $\hat{\boldsymbol{\theta}}$.

Given measurements α_j and ξ_j and uncertainties $\sigma_{\alpha j}$ and $\sigma_{\xi j}$ obtained from fits to the spectra at temperatures T_j, we can obtain the parameters of interest from a fit to the temperature dependence. The ML estimate in this case reduces to a least-squares fit to the parameters $\boldsymbol{\beta}=[\lambda_{tr},T_0,\omega_p,\eta,\tau_1,\ldots,\tau_N]$,

$$\chi^2(\beta) = \sum_j \left\{ \left(\frac{\alpha_j-\hat{\alpha}(\boldsymbol{\beta},T_j)}{\sigma_{\alpha j}}\right)^2 + \left[\frac{\xi_j-\hat{\xi}(\boldsymbol{\beta},T_j)}{\sigma_{\xi j}}\right]^2 \right\}, \tag{7}$$

where the functions $\hat{\alpha}$ and $\hat{\xi}$ return the ideal values of α and ξ for the given parameters.

We have tested our analysis on measurements of thin films of polycrystalline Pb, deposited onto 15 mm diameter c-axis sapphire substrates using thermal evaporation at 10^{-7} Torr. To avoid oxidation and island formation, we deposited thin germanium buffer and capping layers, and cooled the substrates to near 77 K during growth.[13,14] The effect of the germanium buffer and capping layers on the optical properties is negligible.

Figure 1 shows $E_s(t)$ and $|\tilde{E}_s(\omega)|$ for the pulse measured at $T=295$ K, together with the residuals, given by $\tilde{t}_{sr}(\boldsymbol{\theta};\omega_i)\tilde{E}_{ri}-\tilde{E}_{si}$. In real measurements, small amounts of radiation scatter from the sample holder aperture and mix coherently with the main signal; this is apparent in the time-domain fit residuals. Compared with the main signal, this scattered radiation is weighted toward lower frequencies and delayed by about 2 ps. It is approximately independent of temperature, so we treat it as a background,[10] modeling it as an additional term in $\tilde{t}_{sr}$ using an empirically determined rational form $\tilde{t}_{\text{sc}}(\omega)=(b_0+ib_1\omega)/(a_0+i\omega)e^{i\omega\Delta}$, with the delay Δ fixed at 1.8 ps for all temperatures. We further limit the influence of scattered radiation by restricting our fit to frequencies over the range 0.5–1.0 THz, where the main signal dominates.

We reject temperatures that yield $C(\boldsymbol{\theta})$ values outside of the 95% confidence interval for the described F distribution; this leaves 27 temperature points out of a total of 42 measurements. Our sample positioning error is largest at temperatures above 100 K, making these measurements more susceptible to systematic error from scattered radiation, and we find that these fits are rejected with greater frequency. If we insist on achieving values of $C(\boldsymbol{\theta})$ indicative of good fits, we can include more frequencies in the fit only at the expense of choosing a more complicated model for the background, and this produces greater uncertainty in the parameters of interest. In the fits shown, including the background

Downloaded 05 Apr 2006 to 142.58.211.84. Redistribution subject to AIP license or copyright, see http://apl.aip.org/apl/copyright.jsp

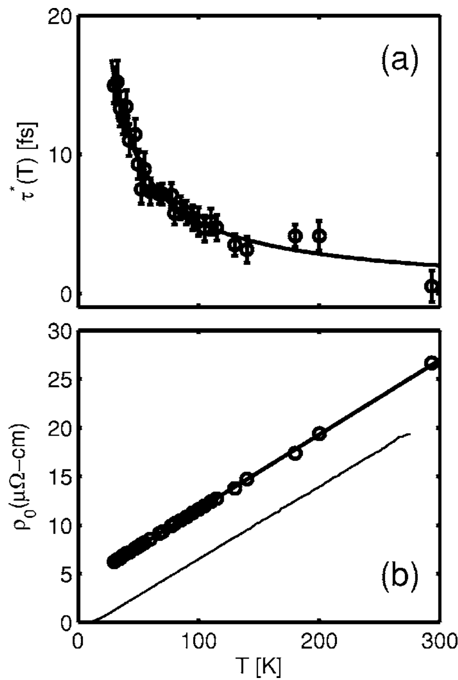

FIG. 2. Eliashberg model fits to TDTS data for (a) the renormalized scattering lifetime τ^* and (b) the dc resistivity ρ_0. The uncertainty in ρ_0 is smaller than the marker size, and the thin line shows bulk single-crystal resistivity for comparison.

term leaves $\xi(T)$ unchanged to within 1 fs, comparable with the statistical uncertainty.

The renormalized relaxation times and dc resistivities obtained from our analysis of the thin films, together with the resistivity of a bulk single crystal,[15] are shown in Fig. 2. The fit parameters are shown in Table I, with uncertainties determined from the curvature of $\chi^2(\boldsymbol{\beta})$. We show unconstrained fits and fits for which λ_{tr} was held fixed at 1.55; the nonlinearity of Eq. (7) in $\boldsymbol{\beta}$ produces strong parameter correlations, so if independent measurements reduce the uncertainty in one parameter, this strongly reduces uncertainty in the others. For the unconstrained fit to T_0 the lower bound is unphysical, which simply means that the distribution of expected values for this parameter is not Gaussian. We have varied the fit range, the background model complexity, the overall delay associated with the background, and the criteria for rejecting points, and in all cases the parameter estimates are consistent with those shown, though sometimes with greater uncertainty. Although the uncertainties are relatively large, our analysis points clearly to avenues for improvement, and if the systematic uncertainty can be reduced below the statistical uncertainty, simulations indicate that our method is capable of providing estimates to two significant figures for all of the quantities shown.

TABLE I. Parameter values and uncertainties obtained from ML fits. Two sets are shown; in one all parameters are free, and in the other λ_{tr} is held fixed. All values are consistent with existing literature, also shown.

Parameter	All free	$\lambda_{tr} \equiv 1.55$	Expected[a]
λ_{tr}	2.0 ± 1.7	1.55	1.55
ω_p (eV)	9.6 ± 2.6	9.5 ± 1.9	9.6
T_0 (K)	26 ± 30	28 ± 10	27

[a]Values include λ_{tr} from tunneling, (Ref. 2) ω_p from band theory, (Ref. 16) and T_0 from tunneling measurements of $\alpha^2F(\omega)$ (Refs. 2 and 17).

The authors acknowledge support from NSERC, the CIAR Program in Quantum Materials, the Sloan Foundation, and the Research Corporation. One of the authors (J.S.D.) acknowledges helpful discussions with J. Bechhoefer and R. Lockhart.

[1]G. Grimvall, *The Electron-Phonon Interaction in Metals* (North-Holland, Amsterdam, 1981).
[2]W. L. McMillan and J. M. Rowell, in *Superconductivity*, edited by R. D. Parks (Marcel Dekker, New York, 1969).
[3]B. Farnworth and T. Timusk, Phys. Rev. B **14**, 5119 (1976).
[4]M. C. Nuss and J. Orenstein, in *Millimeter and Submillimeter Wave Spectroscopy of Solids*, edited by G. Grüner (Springer, Berlin, 1998), pp. 7–50.
[5]P. B. Allen, Phys. Rev. B **3**, 305 (1971).
[6]W. Götze and P. Wölfle, Phys. Rev. B **6**, 1226 (1972).
[7]S. V. Shulga, *Proceedings of the NATO Advanced Study Institute on High-T_c Superconductors and Related Materials* (Kluwer, Dordrecht, 2001), pp. 323–360.
[8]R. E. Prange and L. P. Kadanoff, Phys. Rev. **134**, A566 (1964).
[9]G. E. P. Box, G. M. Jenkins, and G. C. Reinsel, *Time Series Analysis: Forecasting and Control*, 3rd ed. (Prentice Hall, Englewood Cliffs, 1994).
[10]R. J. Barlow, *Statistics: A Guide to the Use of Statistical Methods in the Physical Sciences* (Wiley, Chichester, 1989).
[11]J. Schoukens, R. Pintelon, and J. Renneboog, IEEE Trans. Instrum. Meas. **37**, 10 (1988).
[12]I. Kollár, IEEE Trans. Instrum. Meas. **42**, 2 (1993).
[13]R. H. Willens, A. Kornblit, L. R. Testardi, and S. Nakahara, Phys. Rev. B **25**, 290 (1982).
[14]A. V. Silhanek, S. Raedts, and V. V. Moshchalkov, Phys. Rev. B **70**, 144504 (2004).
[15]L. A. Hall, Natl. Bur. Stand. (U.S.) Tech. Note (U.S. GPO, Washington, D.C., 1968), Vol. 635.
[16]O. Rapp, B. Sundqvist, and J. Neve, Phys. Rev. B **32**, 2200 (1985).
[17]A. V. Puchkov, D. N. Basov, and T. Timusk, J. Phys.: Condens. Matter **8**, 10049 (1996).

Downloaded 05 Apr 2006 to 142.58.211.84. Redistribution subject to AIP license or copyright, see http://apl.aip.org/apl/copyright.jsp